

## **General Disclaimer**

### **One or more of the Following Statements may affect this Document**

- This document has been reproduced from the best copy furnished by the organizational source. It is being released in the interest of making available as much information as possible.
- This document may contain data, which exceeds the sheet parameters. It was furnished in this condition by the organizational source and is the best copy available.
- This document may contain tone-on-tone or color graphs, charts and/or pictures, which have been reproduced in black and white.
- This document is paginated as submitted by the original source.
- Portions of this document are not fully legible due to the historical nature of some of the material. However, it is the best reproduction available from the original submission.

# NASA TECHNICAL MEMORANDUM

NASA TM X-64927

(NASA-TM-X-64927) A DIGITAL ALGORITHM FOR  
SPECTRAL DECONVOLUTION WITH NOISE FILTERING  
AND PEAK PICKING: NOFIPP-DECON (NASA) 41 p  
HC \$3.75 CSCI 09B

N75-24383

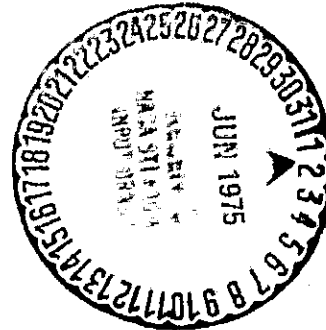
Unclas  
21797

G3/61

## A DIGITAL ALGORITHM FOR SPECTRAL DECONVOLUTION WITH NOISE FILTERING AND PEAK PICKING—NOFIPP-DECON

By Thomas R. Edwards, Gray L. Settle,  
and Randall D. Knight

February 1975



**NASA**

*George C. Marshall Space Flight Center  
Marshall Space Flight Center, Alabama*

1. REPORT NO. NASA TM X-64927		2. GOVERNMENT ACCESSION NO.		3. RECIPIENT'S CATALOG NO.	
4. TITLE AND SUBTITLE A Digital Algorithm for Spectral Deconvolution with Noise Filtering and Peak Picking—NOFIPP-DECON				5. REPORT DATE February 1975	
				6. PERFORMING ORGANIZATION CODE	
7. AUTHOR(S) Thomas R. Edwards, Gray L. Settle,* and Randall D. Knight†				8. PERFORMING ORGANIZATION REPORT #	
9. PERFORMING ORGANIZATION NAME AND ADDRESS George C. Marshall Space Flight Center Marshall Space Flight Center, Alabama 35812				10. WORK UNIT NO.	
				11. CONTRACT OR GRANT NO.	
12. SPONSORING AGENCY NAME AND ADDRESS National Aeronautics and Space Administration Washington, D. C. 20546				13. TYPE OF REPORT & PERIOD COVERED Technical Memorandum	
				14. SPONSORING AGENCY CODE	
15. SUPPLEMENTARY NOTES Prepared by Space Sciences Laboratory, Science and Engineering *Systems Dynamics Laboratory, Marshall Space Flight Center †Physics Department, University of California, Berkeley					
16. ABSTRACT NOFIPP-DECON is an acronym representing software logic performing Noise-Filtering, Peak-Picking Deconvolution. The basic concepts involved are multiple convoluted convolute integers and multiparameter optimization pattern search. A brief description of the two theories is followed by a detailed discussion of the three aspects of the software package.  NOFIPP-DECON has been applied to a number of experimental cases ranging from noisy, nondispersive X-ray analyzer (multichannel) data to very noisy photoelectric polarimeter data. Comparisons have been made with published infrared data, and a man-machine interactive language has evolved for assisting in very difficult cases (using a graphics interactive terminal). A modified version of the program is being used for routine preprocessing of mass spectral and gas chromatographic data.  The entire logic works rather rapidly from the point of view of most experiments, processing approximately 12 peaks per minute. The program fits comfortably in an 8K minicomputer (16K with interactive graphics).					
17. KEY WORDS			18. DISTRIBUTION STATEMENT  Unclassified - Unlimited  <i>Thomas R. Edwards</i>		
19. SECURITY CLASSIF. (of this report) Unclassified		20. SECURITY CLASSIF. (of this page) Unclassified		21. NO. OF PAGES 41	
				22. PRICE NTIS	

## ACKNOWLEDGMENTS

The authors wish to express their gratitude to Helmut Schwille, a former National Academy of Sciences postdoctoral resident research associate, for supplying the proportional counter data from his High Energy Astronomy Observatory experiment; Lowell M. Schwartz of the University of Massachusetts for his spectrum of potassium squarate; and Alan Gary of the Space Sciences Laboratory of the Marshall Space Flight Center for supplying his very noisy polarimeter data.

## TABLE OF CONTENTS

	Page
INTRODUCTION . . . . .	1
NOISE . . . . .	1
THE THEORY OF CONVOLUTING INTEGERS . . . . .	2
Nature of the Filter . . . . .	3
Convolution . . . . .	3
Convolute Integers . . . . .	4
Double Convolution . . . . .	6
PEAK PICKING . . . . .	7
DECONVOLUTION . . . . .	8
Pattern Search . . . . .	8
Constraints . . . . .	11
APPLICATION TO SPECTRAL PROBLEMS . . . . .	11
Flow Chart . . . . .	11
Experimental Results . . . . .	12
CONCLUSIONS . . . . .	30
APPENDIX . . . . .	33
REFERENCES . . . . .	36

## LIST OF ILLUSTRATIONS

Figure	Title	Page
1.	Hooke and Jeeves algorithm 5-part logic . . . . .	9
2.	Synthetic mass spectrum — smoothing and peaks . .	13
3.	Synthetic mass spectrum — deconvolution . . . . .	14
4.	HEAO proportional counter noise . . . . .	15
5.	HEAO proportional counter shoulder . . . . .	16
6.	Potassium squarate man-machine interaction . . . .	18
7.	Potassium squarate deconvolution . . . . .	19
8.	HEAO proportional counter excessive peaks . . . .	20
9.	HEAO proportional counter deconvolution . . . . .	21
10.	Polarimeter excessive noise . . . . .	22
11.	Polarimeter curve fitting . . . . .	23
12.	HEAO proportional counter deconvolution . . . . .	24
13.	HEAO proportional counter deconvolution . . . . .	25

## TECHNICAL MEMORANDUM X-64927

### A DIGITAL ALGORITHM FOR SPECTRAL DECONVOLUTION WITH NOISE FILTERING AND PEAK PICKING — NOFIPP-DECON

#### INTRODUCTION

NOFIPP-DECON is an acronym for a software package which performs the following functions:

- (1) Noise Filtering (smoothing data)
- (2) Peak Picking (location of spectral peaks and shoulders)
- (3) Deconvolution (unfolding overlapping spectral peaks)

The algorithms are the result of the application of Savitzky and Golay's convolute integers and Hook and Jeeves' multiparameter optimization pattern search. The software works rather fast from the viewpoint of the computer time domain and is applicable to a number of diverse problems, some of which will be discussed in detail. The output information is oriented about a graphics display unit which can be utilized for a man-machine interaction, and this has been done for a few difficult problems.

This report will discuss the three distinct aspects of NOFIPP-DECON, indicate the nature of the software, and present the results of a number of test cases. A flow chart is presented as an appendix. A brief description of the theory of convolute integers and pattern search will be presented to clarify the logic used in the software algorithm.

#### NOISE

Most experimentalists are deeply concerned with the problem of noise associated with the data that computers receive from the experimental world. This concern arises because much information from an experiment may be lost as a result of a poor signal-to-noise ratio. The source of this unwanted noise is usually a combination of ground loops, transient currents, reading errors, or using equipment at the limits of its range. In most experiments, the noise can be assumed to be a random event distributed normally about the true signal. This is a

Gaussian-shaped distribution, with most of the deviations caused by noise occurring within one standard deviation of the signal. One can usually assume that the standard deviation of the noise is independent of the signal value and is also constant throughout the experiment.

Under such assumptions, it is possible to utilize several techniques for enhancing the signal-to-noise ratio. An example is the simple RC filter used to remove the high-frequency noise component from an analog signal. However, analog hardware filters do not satisfactorily reduce all the noise before the analog signal is digitized [1]. Unfortunately, the noise present in the analog signal carries over into the digital world. Thus, the need arises for a digital filter which is capable of complementing the signal-to-noise enhancement which took place in the analog world. Several of these filters exist [2-4], notably those resulting from linear operator theory, such as the fast Fourier transform. This report will describe the application of a filter resulting from regression calculations, least squares theory. The theory behind this filter can be found in some texts that cover regression calculations for equal interval data, but Savitzky and Golay in 1964 [5] understood the power of these calculations from the viewpoint of convolving the data with a weighting function in the computer. They developed a universal set of numbers known as convolute integers. As a result of the application of the convolute integers, smoothing and higher order derivatives are available from a very fast algorithm. These convolute integers have been applied to develop a fast digital noise filter capable of locating spectral peaks and shoulders.

## THE THEORY OF CONVOLUTING INTEGERS

The theory of convolute integers is well described by Savitzky and Golay, and a recent correspondence by Steinier, et al. [6] points out a minor correction to the theory. The following sections will describe (1) the nature of the filter, i.e., the naiveté of its application; (2) the relationship between convoluting experimental data with a weighting function which leads to the nomenclature convolute integers; (3) the theory with emphasis on convoluting convoluted data; and (4) a number of test and actual cases indicating the flow of logic and power of the technique in noisy experimental data.



## Nature of the Filter

The nature of the filter is that of a moving smoothing average, equations (1) and (2). The  $j$ th data point ( $Y_j$ ) is modified by the  $2m+1$  points of which it is the center:

$$Y_j^* = \sum_{i=-m}^m C_i Y_{j+i} / N \quad (1)$$

$$Y_{10}^* = C_{-3} Y_7 + C_{-2} Y_8 + C_{-1} Y_9 + C_0 Y_{10} + C_{+1} Y_{11} + C_{+2} Y_{12} + C_3 Y_{13} / N \quad (2)$$

For the moving smoothing average, the coefficients  $C_i$  are integers which are equal to unity, and  $N$  is the normalization factor equal to  $2m+1$ . By allowing  $j$  to run through the index of the array, the data are smoothed using only simple arithmetic averaging operations. It is clear that  $m$  can be set to any value, giving a  $2m+1$  point filter. It is important to clearly state that raw data points must be held in the filter at all times; otherwise the filter will be smoothing already smoothed data points (a recursive type filter). Equation (1) shows that the filter operates by modifying a given point to be some function of itself and its nearest neighbors. An RC filter can use only past information, and this introduces a unidirectional distortion into the data; i. e., phase shift. The digital filter, however, takes advantage of a stored array of data to utilize both past and future points, thus providing an undistorted filter. Using the building blocks of present-day digital logic, those who are hardware oriented can see how well this type logic can be implemented into small, special purpose mini-logic boxes. The logic of a moving smoothing average can be applied to smoothing by application of a cubic equation to seven points or obtaining the first derivative of a quintic by using nine points.

## Convolution

The  $C_i$  coefficients are called convoluting integers because the filter can be considered an operator which forms the smoothed data  $Y^*(t)$  by integrating the raw data  $Y(t)$  with a weighting function  $w(t)$ . Since the weighting at a point depends upon the time difference between the weighted point and the point being smoothed, the filtering operation can be written as

$$Y^*(t) = \int w(\tau) Y(t - \tau) d\tau \quad (3)$$

This integral is defined as the convolution to  $Y(t)$  with  $w(t)$ . In a digital filter the weighting function is of the form

$$w(\tau) = \sum_{i=-m}^m C_i \delta(\tau + i) / N \quad (4)$$

where  $\delta(t)$  is the Dirac-delta function representing the discrete sampling of the data. Using this in equation (3) at time  $t = j$  gives

$$\begin{aligned} Y^*(j) &= \int \left[ \sum_{i=-m}^m C_i \delta(\tau + i) / N \right] Y(j - \tau) d\tau \\ &= \sum_{i=-m}^m C_i Y(j + i) / N \end{aligned} \quad (5)$$

By equating  $Y(j + i)$  with  $Y_{j+i}$ , equation (5) is seen to be identical to equation (1). Thus, the  $C_i$ 's are known as convoluting integers.

### Convolute Integers

While the moving smoothing average works well for a quasi-dc signal, it tends to drastically distort a curve of large curvature, such as a peak. Thus, one would like to retain the simplicity of equation (1) but find a set of convoluting integers which does not alter the shape of the data. The most commonly used method for smoothly fitting a curve to a group of data points is the method of least squares; therefore, one is led to try fitting an  $n$ th degree polynomial to  $2m + 1$  points such that the sum of the squares of the residuals is minimized. The goal is to express the polynomial value at the center point of the curve in terms of the  $2m + 1$  unsmoothed nearest neighbors and then regard the polynomial center point as the smoothed value of data. This method will be seen to provide not only a set of convoluting integers for smoothing, but also for finding the first  $n$  derivatives, following the format of a moving smoothing average.

Two assumptions concerning the data must be met if the filter is to be effective: the data must occur at equally spaced intervals along the abscissa, and the curve formed by the data in the filter must be reasonably smooth [5]. The first of these assumptions is always met in computer work because the abscissa is actually the time interval at which the data are sampled, and this is equal interval and stable to 0.01 percent accuracy or better. The second assumption is satisfied if the analog-to-digital conversion rate is adequate for the frequencies involved in the experimental data. A comfortable rule of thumb indicates a sampling rate of at least five times the frequency of the signal.

This report will deal primarily with the filtering of the intensity since it is the noisiest signal in spectroscopy. The problem is to fit a polynomial to  $2m+1$  points and then replace the center point by its polynomial, or smoothed value. Since the data points are assumed to be uniformly spaced and odd in number, they can be normalized and centralized to be integer values centered at zero [7]; the  $n$ th degree polynomial is then of the form

$$Y_i^* = \sum_{k=0}^n b_k i^k \quad -m < i < m \text{ integers values} \quad (6)$$

$$= b_0 + b_1 i + \dots + b_n i^n$$

The value at  $i = 0$ , the center point, is all that is required; therefore, clearly  $Y_0^* = b_0$ . The smoothed value at a point is merely the first coefficient of the best-fit polynomial centered at the point. By taking derivatives of the polynomial, one can show

$$Y_0^* = b_0$$

$$\frac{dY_0^*}{dt} = \frac{dY_0^*}{di} \frac{di}{dt} = \frac{1}{\Delta t} \frac{df_0}{di} = \frac{b_1}{\Delta t} \quad (7)$$

•  
•  
•

$$\frac{d^s Y_o^*}{dt^s} = \frac{dY_o^s}{dt} \frac{1}{(\Delta t)^s} \frac{ds f_o}{di^s} \frac{s! b_s}{(\Delta t)^s}$$

where  $\Delta t$  is the constant step size between abscissa points; i.e., the analog-to-digital conversion time. Thus, the smoothed value at the first  $n$  derivatives at the center point can be found by solving for the proper regression coefficients.

The solution for the regression coefficients  $b_s$  can be found in numerous texts on regression analysis and will not be given here. One can show that the solution is of the form

$$s! b_s = \sum_{i=-m}^m C_i Y_i / N \quad (8)$$

This is identical to equation (1), with  $j=0$ , since the points here are centralized. Thus, each  $b_s$  and, hence, each derivative can be evaluated by a set of  $C_i$  convoluting integers and a normalizing constant  $N$ . These integers depend on the order of derivatives (0 to  $n$ ), the number of points ( $2m+1$ ), and the order of the polynomial ( $n \leq 2m+1$ ). Large tables of these convoluting integers with their corresponding normalization factors can be found in References 5 and 8.

### Double Convolution

The real power of this technique comes from the ability to simultaneously convolute already convoluted data. This gives one filter the ability to perform more than one operation simultaneously. Convoluting two sets of integers results in a single set of integers which performs the operations of the two original filters simultaneously. This is decidedly advantageous for programming. Thus, if a  $2m+1$  point  $n$ th order smooth is convolved with a  $2p+1$  point  $k$ th order  $s$ th derivative, the results are

$$\frac{d^s Y^*}{dt^s} = \frac{1}{N_s (\Delta t)^s} \sum_{i=-p}^p C_{i,s} \frac{1}{N_o} \sum_{j=-m}^m C_{j,o} Y_{i+j} \quad i+j = \text{constant}$$

$$= \frac{1}{N_o N_s (\Delta t)^s} \sum_{i=-p}^p \sum_{j=-m}^m C_{i,s} C_{j,o} Y_{i+j} \quad (9)$$

$i+j = \text{constant}$

$$= \frac{1}{N} \sum_{h=-(m+p)}^{m+p} d_h Y_h$$

where

$$d_h = \sum_{\substack{i,j \\ i+j=h}} C_{i,s} C_{j,o}$$

$$N = N_o N_s (\Delta t)^s$$

The  $C_{i,s}$ 's are the convoluting integers of the  $k$ th order derivatives, the  $C_{j,o}$ 's are those of the  $n$ th order smooth, and the  $d_h$ 's are those for the combined operations. The resulting filter has  $2(m+p)+1$  points.

### PEAK PICKING

Peak picking entails the location of both peaks and shoulders in the noisy experimental data. All peaks and shoulders are obtained by searching for zero crossings in various order derivatives. The beauty of the convolute integers lies in their ability to double convolute simultaneously. Since taking higher order derivatives is equivalent to a high-pass filter and enhances the noise content of the data, by themselves higher order derivatives make location of zero crossing more difficult; but smoothing, which is equivalent to a low-pass filter, can be performed simultaneously while taking of higher order derivatives and results in a band-pass filter in the sense of linear operator theory. Double convolution of the data, a derivative with a smooth, results in band-pass filtering and allows for unambiguous determination of zero crossings. A more detailed description of the flow chart indicates the use of double convolution.

## DECONVOLUTION

The ability to unfold overlapping spectra or to curve fit complicated transcendental expressions will be described under the heading of deconvolution. For a spectrometer with finite resolution, these methods allow a practical realization of clearly resolving overlapping peaks and shoulders. For a polarimeter, these methods allow a fast and easy method for abstracting all the pertinent data from what may be considered a complicated analytical expression. In either case the problem reduces to curve fitting an analytical expression where a number of parameters are allowed to vary in such a manner as to produce optimal values based upon some user-specified criterion function; i.e., least squares.

The Hooke and Jeeves algorithm [8] is a pattern-search approach toward optimizing an N-dimensional vector by satisfying a criterion function. As such, the algorithm is ideally suited to optimizing the parameters associated with deconvolution.

### Pattern Search

The algorithm can be described as a 5-part logic (Fig. 1). First, an effective criterion function must be established. A criterion function is, by definition, any mathematical representation which is related to all the parameters in such a fashion that a bad set of parameters will increase the criterion function while a good set of parameters will decrease this function, or vice versa. The condition of least squares is the criterion function in a multiparameter regression problem. Whereas regression calculations are algebraic and allow the optimum parameters to be obtained from a solution of a set of normal equations, no such calculus is available for transcendental expressions. However, the least squares condition is applicable to a transcendental expression if one assumes a normal distribution of data. Therefore, the criterion function in this multiparameter search algorithm will be established as a minimization of the root-mean-square deviation resulting from the transcendental expression and the experimental data.

In any search problem, a starting point must be established. The better the starting point, the quicker a solution is reached. Therefore, as much logic as possible should go into establishing good initial values for the parameters. Good beginnings require algorithms which are usually unique to each problem and can be the determining factor in the

# **HOOKE AND JEEVES ALGORITHM**

## **FIVE PART LOGIC**

1. ESTABLISHMENT OF AN EFFECTIVE CRITERION FUNCTION.
2. ESTABLISHMENT OF A STARTING POINT.
3. INITIALIZATION OF STEP SIZE.
4. EXPLORATION ALONG EACH AXIS IN THE N-DIMENSIONAL SPACE.
5. ESTABLISHMENT OF A PATTERN OF MOVEMENT.

## **LOGICAL FLOW CHART**

### **INITIALIZATION**

#### **CRITERION FUNCTION**

#### **BASE POINT**

#### **STEP SIZE**

### **EXPLORATORY MOVES**

#### **ADVANCE**

#### **RETREAT**

#### **STATIONARY**

### **PATTERN MOVES**

#### **VECTOR DISPLACEMENT**

#### **FINAL POINT**

Figure 1. Hooke and Jeeves algorithm 5-part logic.

time required for the pattern search to be effective. The convolute integer technique of locating peaks and shoulders in conjunction with noise filtering has proven quite effective in most of these applications.

The third part of the logic is concerned with the step size associated with each parameter. The step size determines the length of the move that the parameter is allowed to make in advancing toward its optimum value. The initial value of the step size for each parameter can be determined in the following manner. If the initial parameter is known accurately to two significant digits, variations considered will be from the third digit on; then step size 0.9 percent of the initial value would be appropriate. (This allows approximately 100 percent deviation in the third digit.) Care must be exercised not to allow the step size to be a prime factor of the initial parameter or a prime number. Prime step sizes can lead to a zero for an intermediate parameter value, and the search cannot move from such a value.

The last two parts of this 5-part logic are concerned with the search moves. Two types of move are actually involved in the pattern search: exploratory steps and pattern or vector displacements. After the starting point or base point for an iteration has been established, exploratory steps are taken along each axis in the N-dimensional space according to the step size defined for each parameter. This exploration has three possibilities: it may add to or subtract from the value of the parameter or may leave the parameter unchanged.

The decision to change the parameter in either direction or retain its original value depends on which choice lowers the root-mean-square deviation (the value of the criterion function). If the parameter remains unchanged, the step size associated with that parameter is halved and the exploration proceeds along another axis. This reduction in step size represents an increase in sensitivity toward lowering the criterion function. Exploring each axis in this manner and combining the results advances the search from the base point to the midpoint for this iteration and allows a vector direction or a pattern to be established. The vector direction is then determined by the net displacement between the base point and the midpoint. Based on the assumption that whatever constituted a successful exploratory move is likely to do so again, an advance in the established vector direction is made. The net displacement between the current base point and midpoint is added again to the midpoint to obtain the final point for the iteration. This final point is then advanced as far as possible by the net displacement (adding the net



displacement to the final point), always examining the criterion function to assure that the move was good. The major advance toward the optimum values of the parameters for most problems takes place in the pattern moves. When a pattern move goes beyond a good point (indicated by an increase in the root-mean-square deviation), the multiparameter vector retreats to the last good point, which then acts as the base point for a new set of exploratory moves, with the reduced step size.

Thus, from the initial base point to the final optimum values of the parameters, the whole process iterates to produce a lower and lower step size and, subsequently, a minimum in the criterion function. The iteration process can be stopped by any number of conditions; e.g., a fixed number of iterations, a predetermined lowering of the initial root-mean-square value or a control on the number of significant digits allowed in each parameter. The latter condition seems to be the most time consuming.

### Constraints

In addition to good initial values of the parameters, the pattern search needs to be constrained to encourage it to be more efficient. In all these examples a nonnegativity or less than noise level threshold constraint is placed on the ordinate values, and the abscissa is constrained to be within 10 percent of the actual input data. The constraints are checked each time a new value is considered for a parameter prior to calculating the criterion function. In this way the optimization is bounded to a region of acceptable values.

## APPLICATION TO SPECTRAL PROBLEMS

### Flow Chart

Input arguments to the computer subroutine are the usual  $x$  and  $y$ , representing spectral position and intensity, respectively. An additional input argument specifies the noise level below which peaks will not be considered. The actual program has a number of additional options which are indicated by comment cards and user instructions for the software package and will not be mentioned here.

An overview of the logic indicates that the input data are smoothed, peaks and shoulders are considered above a specified noise level, and

their respective  $x$  and  $y$  values are stored in an array. Deconvolution of the stored array is performed according to the criterion function, and a graphic display of the results is viewed and output for hard copy. The ability to see the results in a format compatible with the experimenter's concept of the problem makes understanding and dissemination of the output rather easy and comfortable. This is equivalent to the old wise man's tale that a picture is worth a thousand words. The graphic display gives both the picture and the complementary annotation.

The user is required to specify the criterion function for deconvolution and generate the convolute integers appropriate to the noise in the particular problem. This requires an understanding of the wave forms appropriate to the problem (either analytical or empirical) and an understanding of how to generate convolute integers for a variety of simultaneous operations. The authors are presently preparing comprehensive tables of convolute integers for single and double convolution.

### Experimental Results

Sources of Data. Figures 2 through 13 represent the test cases to which the algorithm has been successfully applied. Figure 2 represents a synthetic mass spectrum to which noise has been added. The root-mean-square value of the noise is approximately 0.12 percent of the maximum peak (No. 4) and 25 percent of the small peak (No. 1). The data were generated at 40 points per amu. Figure 2 is used to demonstrate peak picking and shoulder location. Figure 3 shows the results of applying the optimization logic to deconvolution. In all the figures the dots represent the deconvolved wave forms; the squares represent their linear summation.

Figures 4 and 5 represent some very noisy experimental data resulting from a cosmic ray proportional counter associated with the High Energy Astronomy Observatory (HEAO) experiment and are a good example of applying the noise filter to actual experimental results. The curve on the left of each figure is the raw data, and the one on the right is smoothed, optimized data. The data, recorded on a multichannel analyzer, were produced by radioactive decay of Fe-55. The right peak is the photo peak resulting from ion-pair production in the argon of the detector by 5.9 keV photons produced by K capture in the source. There is also a probability, although considerably less, that the same photons will remove a K electron from the argon, causing the so-called escape peak on the left. The presence of the two peaks is clearly seen in

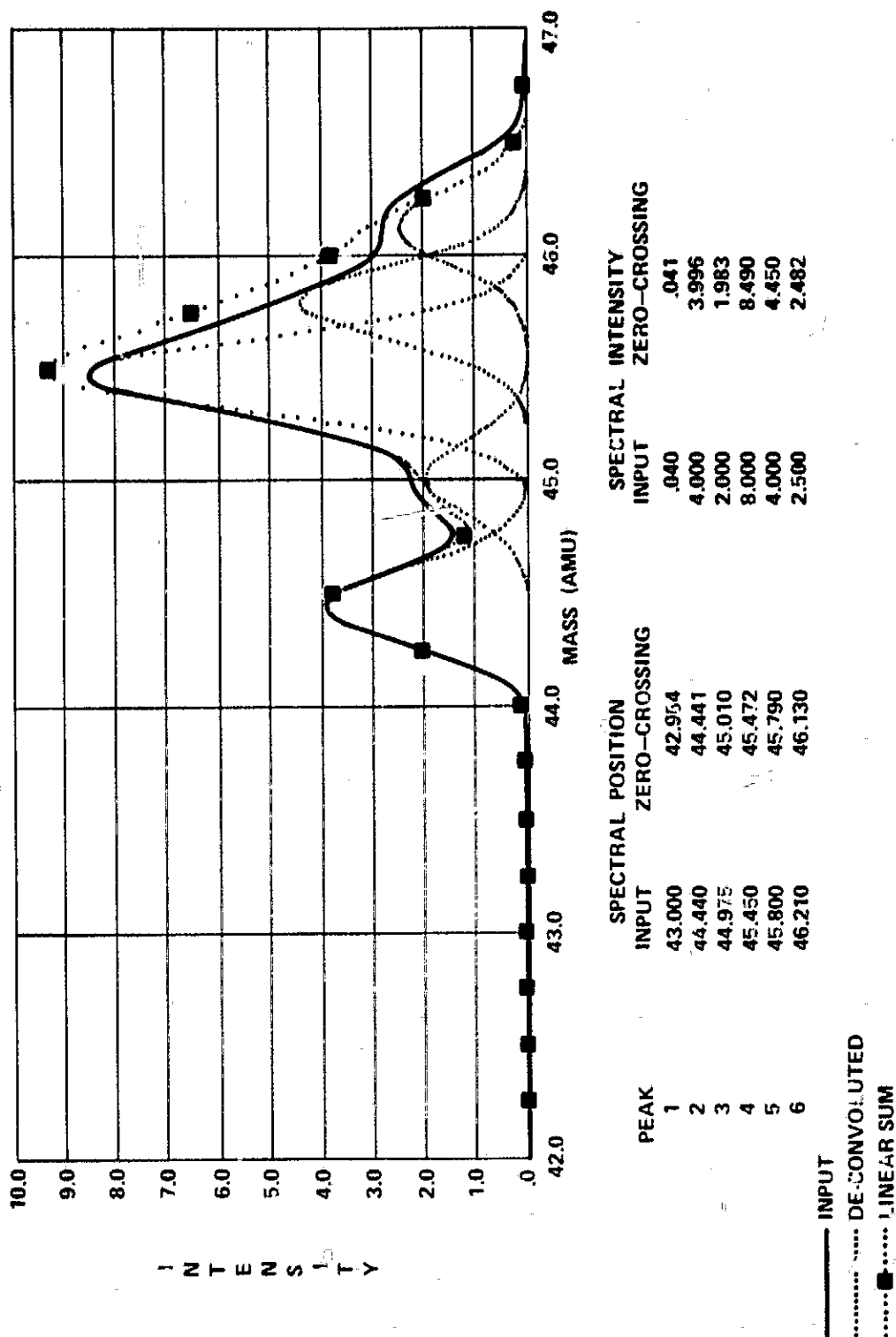


Figure 2. Synthetic mass spectrum — smoothing and peaks.

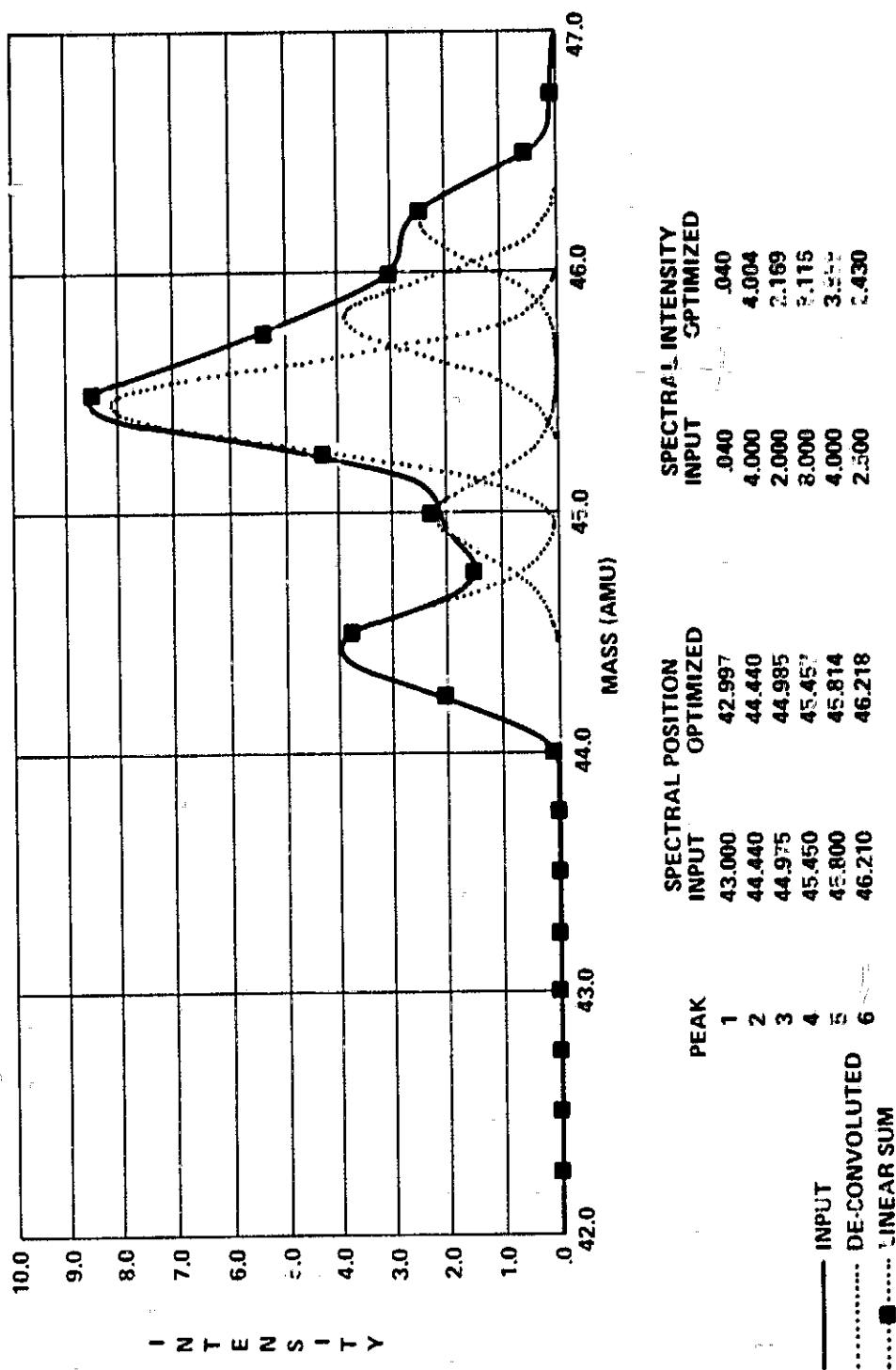


Figure 3. Synthetic mass spectrum — deconvolution.

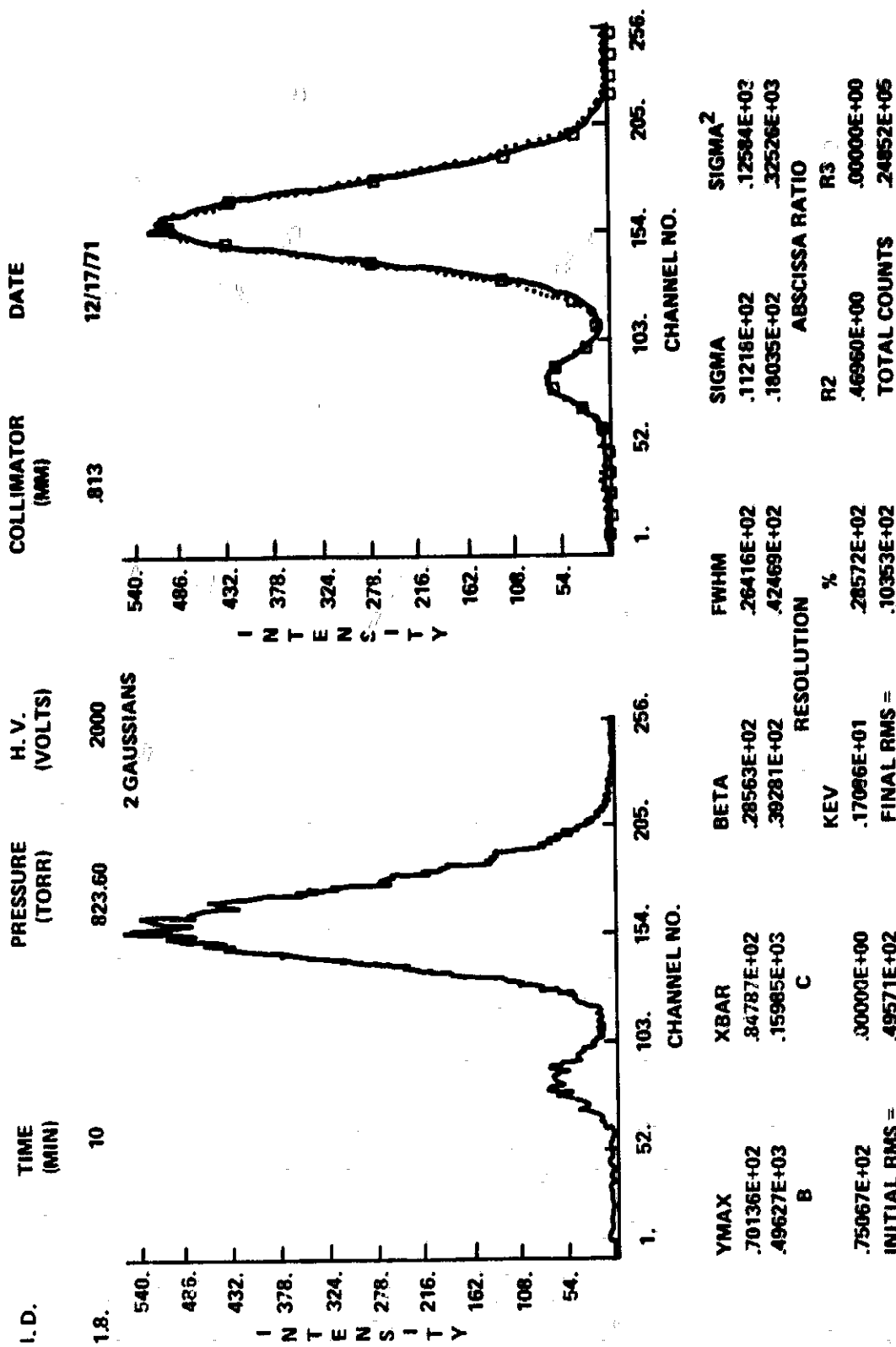


Figure 4. HEAO proportional counter noise.

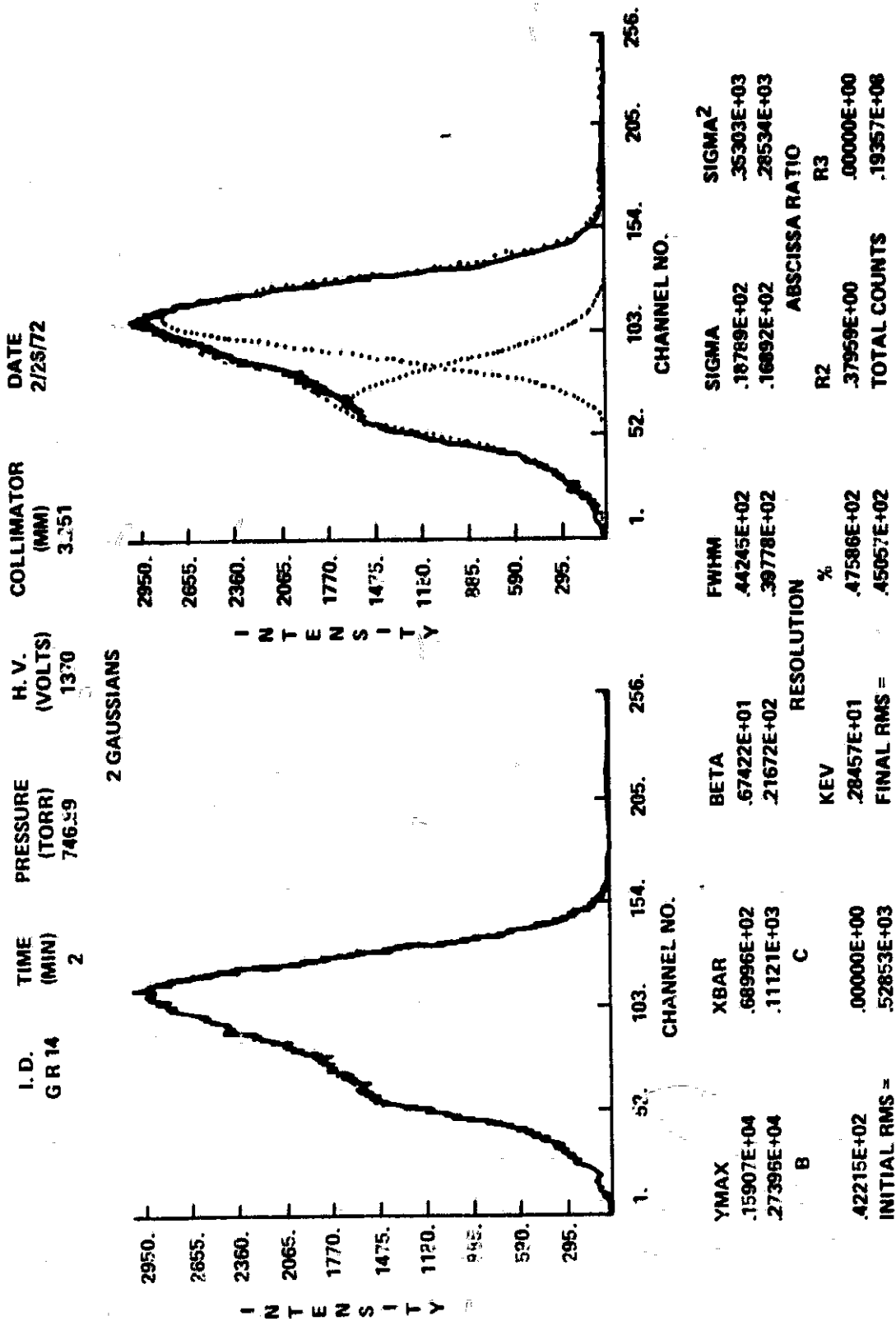


Figure 5. HEAO proportional counter shoulder.

Figures 4 and 5. The data represent a very good experimental test of all aspects of the software.

Figure 6 represents the man-machine interaction in supplying missing information or deleting undesired results. Figures 6 and 7 represent an ultraviolet spectrum of potassium squarate from a Cary 14 spectrophotometer. Figures 8 and 9 represent more of the HEAO data which was rather difficult for the computer to work with by itself.

Figure 10 was obtained from a very noisy multispectral photoelectric polarimeter which requires double convolution noise filter and curve fitting of a complicated analytical expression by optimization. The polarimeter is used in nighttime sky studies of the diffuse interstellar light. The smoothed, optimized curve is the continuous line through the raw data (Fig. 11).

The ability of the graphics display to clearly resolve different physical theories is depicted in Figures 12 and 13. Figure 12 is a theory of all Gaussian wave shapes; Figure 13 represents one Poisson and two Gaussian waves.

Smoothing. All the data that required smoothing were satisfactorily smoothed by a 9-point cubic smooth, equation (10), with the exception of the photoelectric polarimeter data.

$$\begin{aligned}
 \text{Smoothed} & Y(I) = \left\{ -21[Y(I+4) + Y(I-4)] + \right. \\
 \text{output} & \quad 14[Y(I+3) + Y(I-3)] + \\
 & \quad + 39[Y(I+2) + Y(I-2)] + \\
 & \quad 54[Y(I+1) + Y(I-1)] + \\
 & \quad \left. 59[Y(I)] \right\} / 231
 \end{aligned} \tag{10}$$

Note the symmetry in the filter, weighting past and future information equally and present information most strongly.

The polarimeter data required double convolution because of its excessive noise content. Here a 9-point cubic smooth and a 5-point linear smooth were considered simultaneously, resulting in a 13-point filter, equation (11).

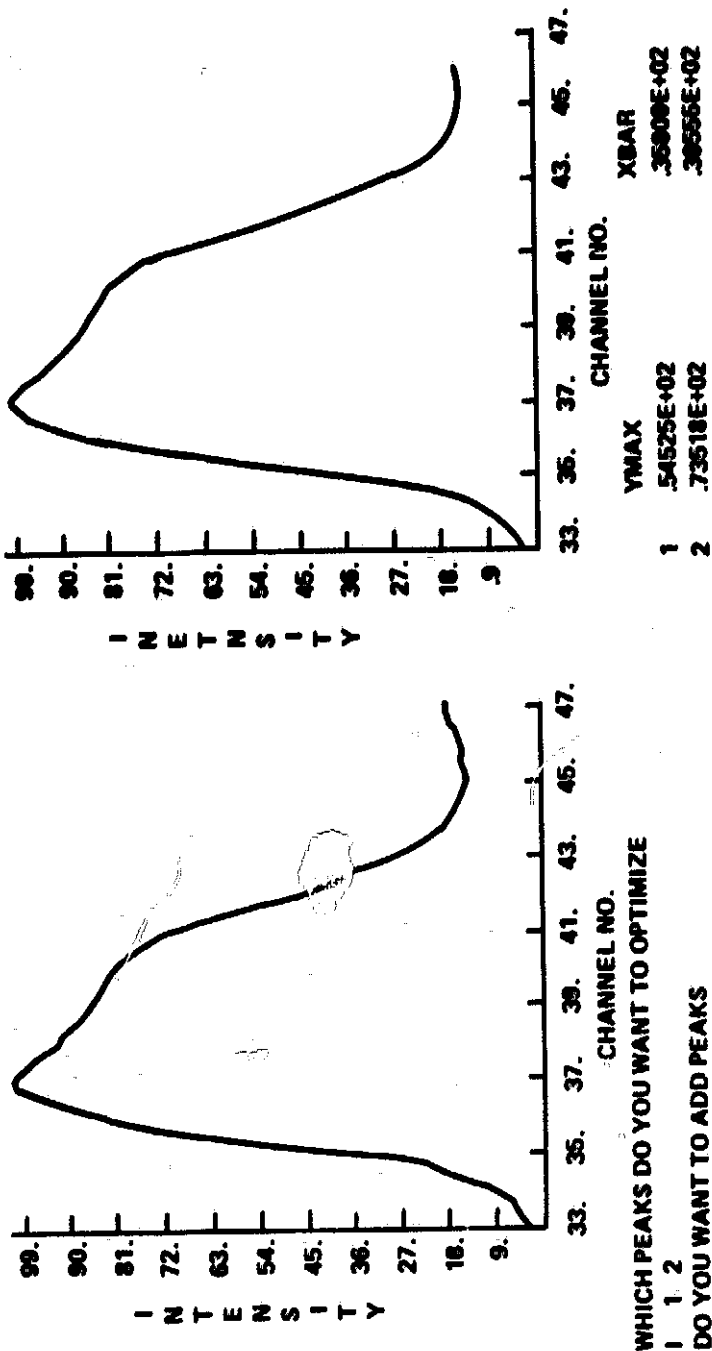
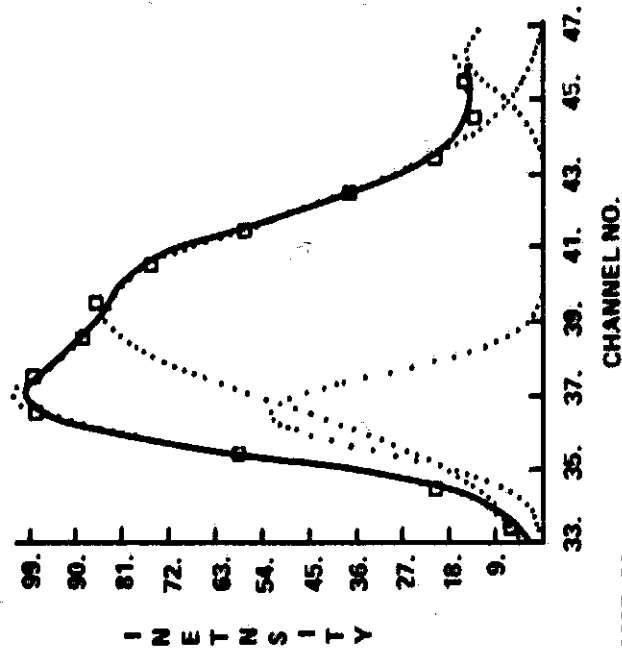


Figure 6. Potassium squarate man-machine interaction.



# SCHWARTZ METHOD OF SPECTRAL PEAK ANALYSIS 4/10/73

3 GAUSSIANS



INITIAL RMS = .19356E+02 FINAL RMS = .14028E+01

AFTER OPTIMIZATION

YMAX	XBAR	BETA
51.19	36.77	1.20
82.52	39.55	2.92
14.78	46.46	1.26

Figure 7. Potassium squarate deconvolution.

I.D. TIME PRESSURE H.V. COLLIMATOR DATE  
(MIN) (TORR) (VOLTS) (MM) 4/19/73

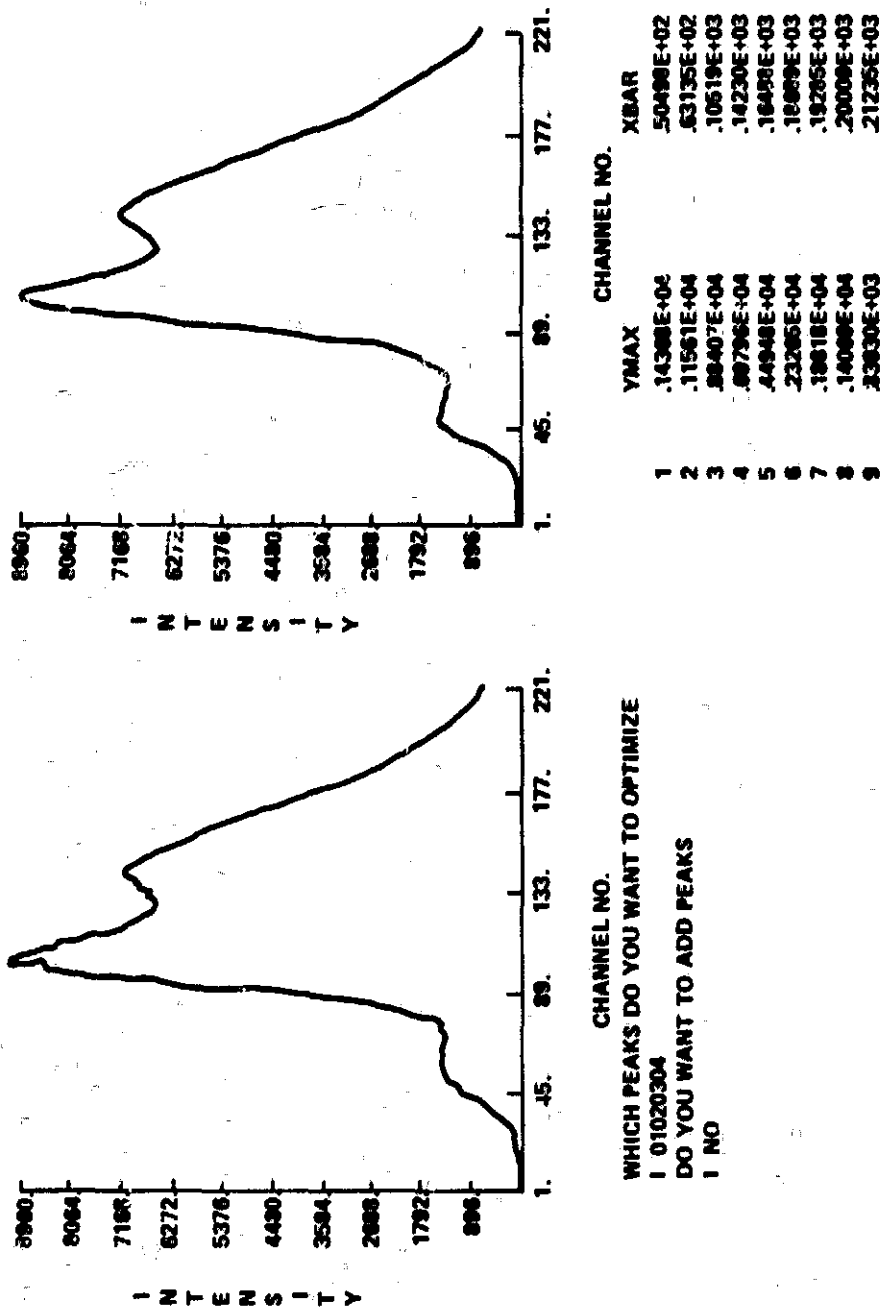
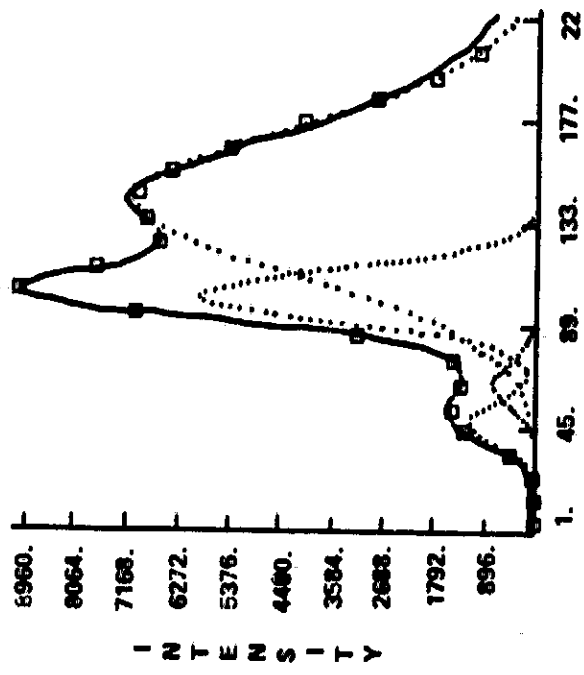


Figure 8. HEAO proportional counter excessive peaks.

I. D.                      TIME                      PRESSURE                      H. V.                      COLLIMATOR                      DATE                      4/19/73                      3.136.2.                      4 GAUSSIANS



YMAX	XBAR	BETA	FWHM	SIGMA	SIGMA <sup>2</sup>
.11728E+04	.47792E+02	.14016E+02	.21257E+02	.90768E+01	.81483E+02
.73124E+03	.65068E+02	.25500E+02	.21456E+02	.91114E+01	.83017E+02
.57271E+04	.10197E+03	.43875E+02	.25633E+02	.10885E+02	.11849E+03
.67659E+04	.14230E+03	.10188E+02	.74234E+02	.31524E+02	.99377E+03
B					
C					
RESOLUTION					
		KEV	%	ABSCISSA RATIO	
.17276E+02	.36899E+02	.37506E+01	.62720E+02	R2	R3
INITIAL RMS =	.14092E+04	FINAL RMS =	.15300E+03	TOTAL COUNTS	
				.56708E+00	
				.73579E+05	

Figure 9. HEAO proportional counter deconvolution.

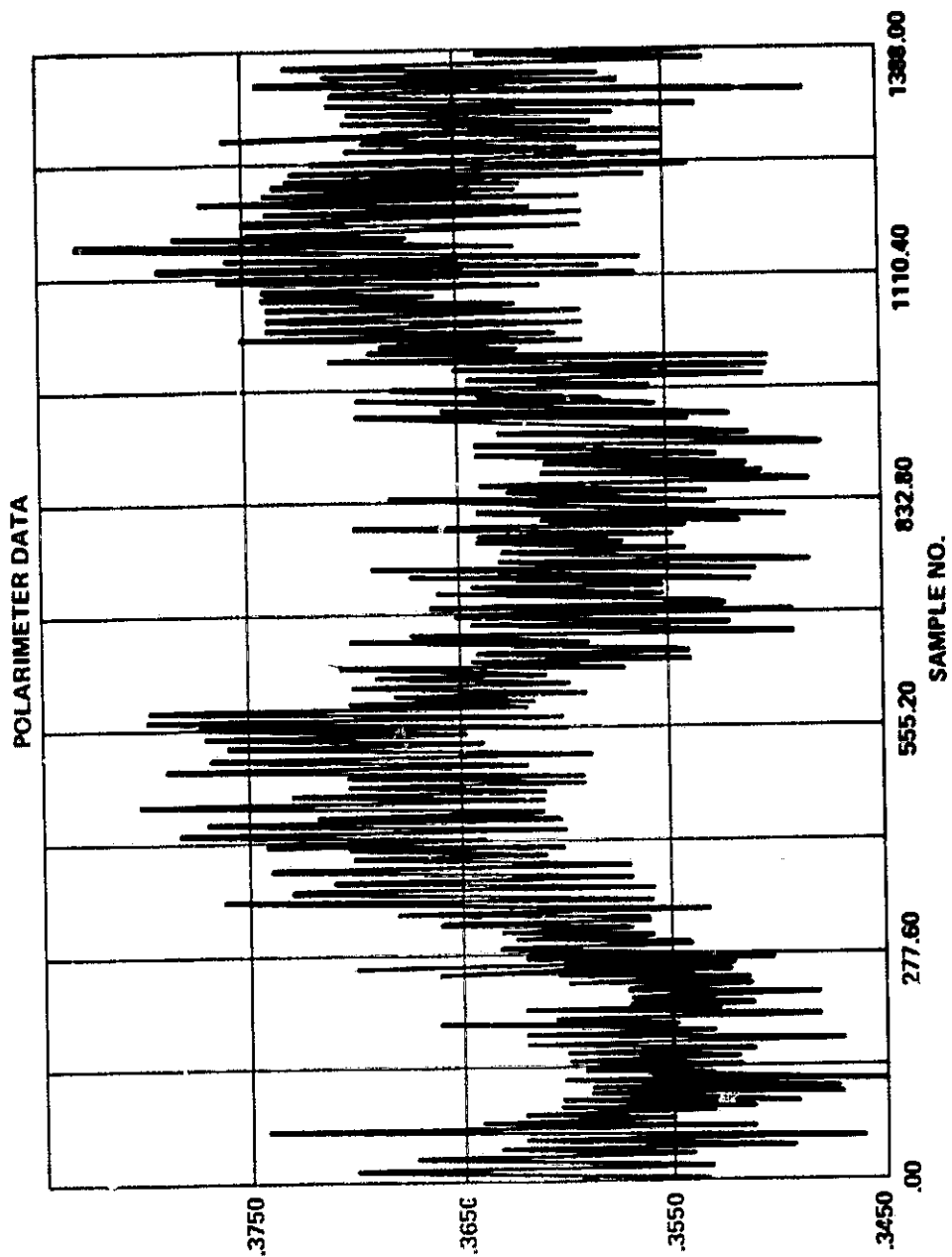
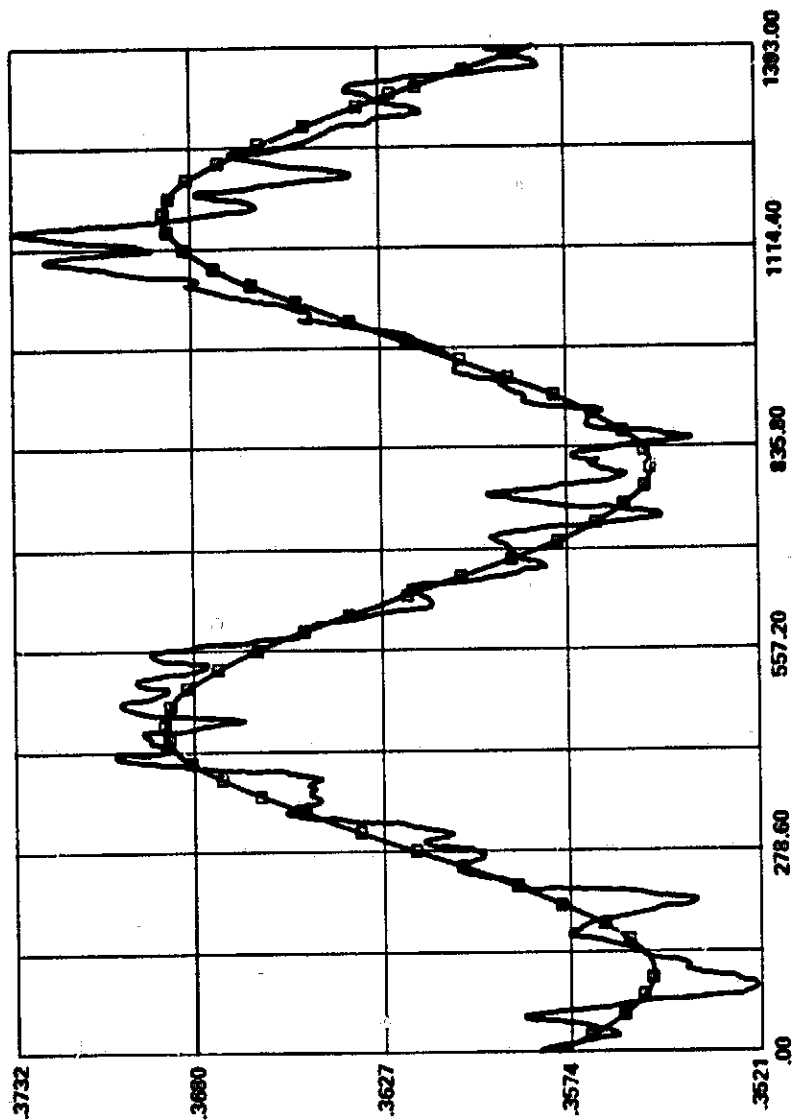


Figure 10. Polarimeter excessive noise.

# POLARIMETER DATA

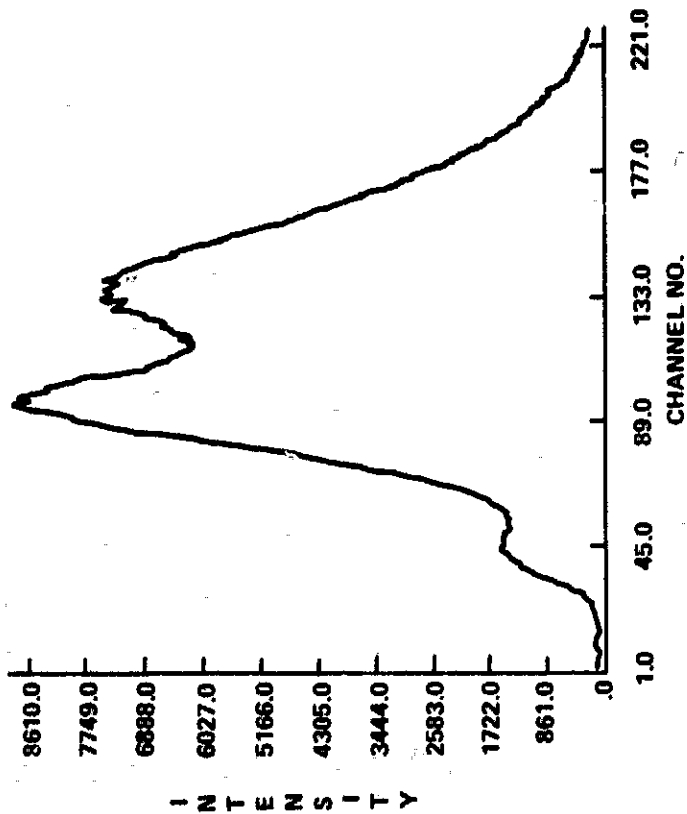


RESULT OF PARAMETER OPTIMIZATION

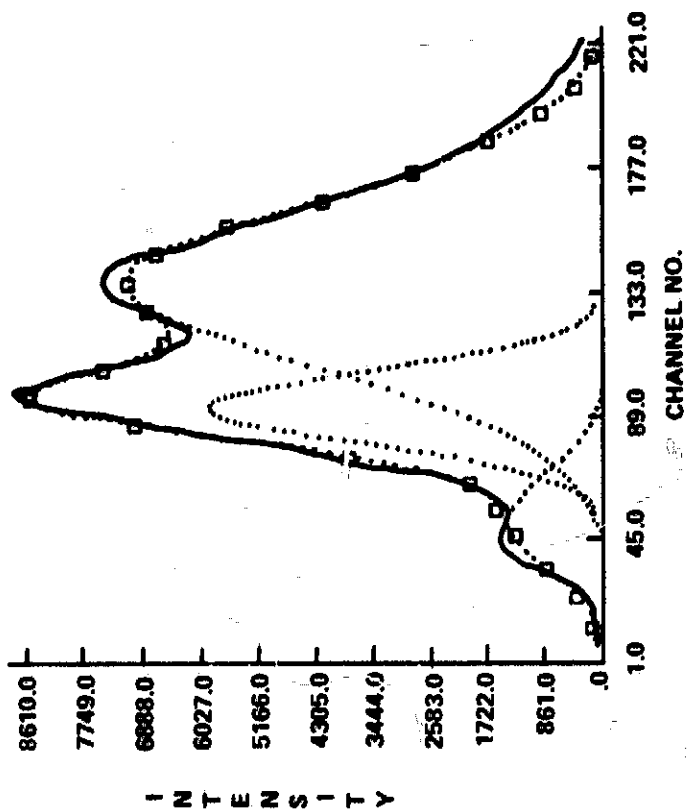
$$Y = .355 + .01 \cos^2 (3.878 T - 5.1734)$$

Figure 11. Polarimeter curve fitting.

3.134.2.



3 GAUSSIANS



YMAX	XBAR	BETA
1344.8433	51.0453	4.8760
5757.2968	90.5471	26.6963
6870.2800	134.2902	10.2712

INITIAL RMS = .1685408E+04  
 FINAL RMS = .2001069E+03

Figure 12. HEAO proportional counter deconvolution.

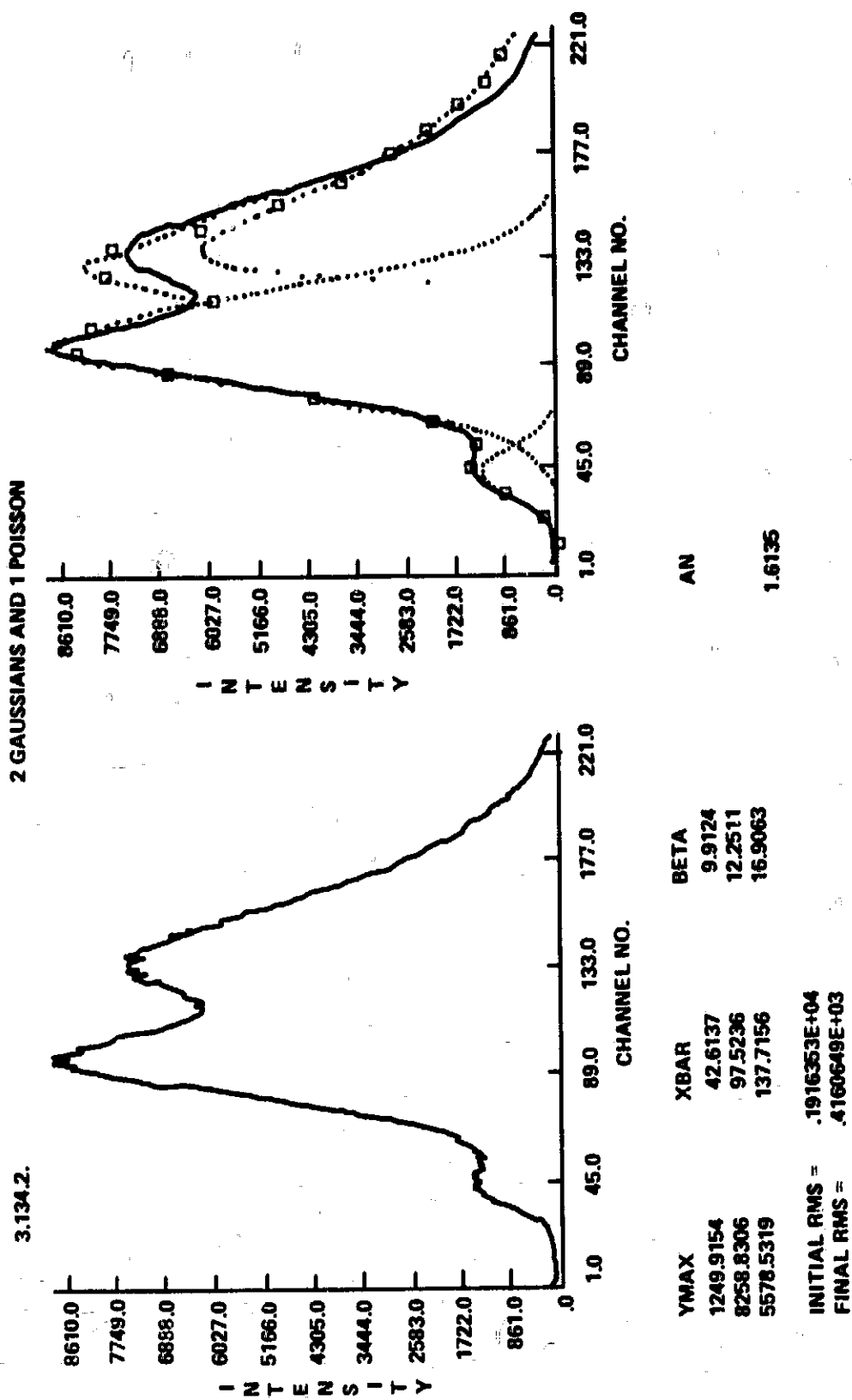


Figure 13. HEAO proportional counter deconvolution.

$$\begin{aligned}
Y(I) = \{ & [Y(I+6) + Y(I-6)] \times -21 \\
& + [Y(I+5) + Y(I-5)] \times -7 \\
& + [Y(I+4) + Y(I-4)] \times 32 \\
& + [Y(I+3) + Y(I-3)] \times 86 \\
& + [Y(I+2) + Y(I-2)] \times 145 \\
& + [Y(I+1) + Y(I-1)] \times 220 \\
& + [Y(I) 245] \} / 1155
\end{aligned}
\tag{11}$$

In all these cases the Y(I) smoothed output is merely placed back into the raw data position of the raw data array, transforming that array into a smoothed data array. The raw data points necessary for the filter are merely held in memory, preventing the filter from becoming recursive in nature (using previously smoothed data points to smooth raw data points). The filter now moves forward a point by shifting Y(I) to Y(I-1) and inputting a new value at the end point in the filter, Y(I+4) for a 9-point cubic smooth.

Peak Picking. Only smoothed data are considered when searching for peaks and shoulders. An 11-point storage vector, YS, contains the smoothed data. To initialize the first 10 points of YS, a 3-point linear average of the first n raw data points is considered, where n is one less than the number of points used in the smoothing filter. YS(11) is then set equal to Y(I), smoothed output, and the filter is now initialized.

If YS(6), the center point of the YS array, is greater than a user-specified noise level below which no peaks will be considered, the filter searches for peaks and shoulders. The first derivative is now found at YS(6). Since taking of a derivative greatly enhances the noise content of the data (i.e., a high-pass filter), the added noise is compensated by a simultaneous linear smooth (i.e., a low-pass filter) which results in a less ambiguous determination of zero crossings (i.e., band-pass filtering). Peaks are found by convolving a 5-point cubic first derivative with a 5-point linear smooth and looking for a zero crossing in the resulting data, DER 1.

$$\begin{aligned}
\text{DER 1} = & 7 (YS_8 + YS_9 - YS_3 - YS_4) \\
& + YS_2 + YS_5 - YS_7 - YS_{10} .
\end{aligned}
\tag{12}$$



The search for zero crossings in the value of DER 1; i.e., sign change, allows one to ignore the normalization factors. To distinguish peaks from valleys, the sign change at the zero crossover must be from positive to negative. Thus, if DER 1 and its product with the derivative at the last point are negative, a peak has occurred between the points and is located by linear interpolation. To prevent any remaining noise from appearing as a peak, the program requires that the intensity rise for at least four consecutive points preceding a peak. Even the smallest of true peaks should easily exceed this if the digital converter sampling rate is adequate for the analog frequencies in question.

Figure 2 shows the results of peak picking on the synthetic test case. Exact values of the five peaks' (No. 1, 2, 3, 4, and 6) spectral positions and spectral intensities are listed under the input columns. The peaks actually found are listed under zero crossings; only peak No. 4 shows a large error, and this was due to an unresolved peak causing a shoulder.

In Figures 4 and 5, special logic was required for combining peaks that were not truly resolved but were the result of excessive noise occurring at the top of the peak. In Figure 5, the small shoulder was determined by the peak picking section of the logic. In Figure 6, the first two peaks were easily determined by the peak picking logic, but a man-machine interaction was required for input of the third peak. Figure 8 is very noisy data which produce an abundance of peaks. Here the program merely requires activation of a sense switch for manual intervention of the data prior to executing the optimization deconvolution logic.

In all the cases, the spectral peaks and positions resulting from the zero crossings are merely stored in a vector which is considered as initial input values for the optimization routines.

Shoulder Locator. The second derivative is found at the same point as the first. Again, the taking of higher order derivatives greatly enhances the noise level, and compensation is obtained by further convolving the derivatives with a linear smooth. Thus, to find the second derivative, DER 2, a 5-point linear smooth is combined with a 7-point cubic second derivative:

$$\begin{aligned} \text{DER 2} = & 5 \text{ YS}_1 + 5 \text{ YS}_2 + 2 \text{ YS}_3 - 2 \text{ YS}_4 - 5 \text{ YS}_5 - 10 \text{ YS}_6 \\ & - 5 \text{ YS}_7 - 2 \text{ YS}_8 + 2 \text{ YS}_9 + 5 \text{ YS}_{10} + 5 \text{ YS}_{11} . \end{aligned} \quad (13)$$

This has the effect of smoothing the data twice without altering the output YS of smoothed data. A shoulder represents a zero crossing in the second derivative, which can be distinguished from other inflection points because the product of the first and third derivatives is positive at shoulders and negative at other zero crossings. Thus, the second derivative is checked for zero crossings in a manner similar to that used for finding peaks. If a zero crossing in this second derivative is found, a 5-point cubic third derivative combined with a 3-point linear smooth is calculated:

$$\text{DER 3} = -\text{YS}_3 + \text{YS}_4 + \text{YS}_5 - \text{YS}_7 - \text{YS}_8 + \text{YS}_9 . \quad (14)$$

The product DER 1  $\times$  DER 3 then determines whether a shoulder has been found. The intensity at this point is misleading because of the influence of the larger peak nearby. Practice has shown that 90 percent of the intensity is a reasonable guess as to the true peak height. With exceptionally poor data, even the doubly convoluted smoothing is often not enough to offset the sensitiveness of the shoulder finder, and erroneous shoulders may be located. To overcome this, it may be necessary to expand the number of points in the filter and perform an additional linear smooth before finding the second derivative.

Figure 3 represents the action of the shoulder locator acting on spectral peak No. 5. Figure 5 looks as if the shoulder locator found the small peak, but close scrutiny of this particular case indicated that this was a peak.

The shoulders are treated in the same fashion as peaks and loaded as they occur into the storage array for input to the optimization routine.

Man-Machine Interaction. By activation of a sense switch, a man-machine interaction can occur prior to executing the deconvolution aspect of the program. Questions are asked the user which allow him to delete, modify, or add peaks and shoulders manually. Upon completion and display of the deconvolution, the user is asked if he is satisfied with the results or wishes to remodify the results. The program then asks for the next set of data. The interactive ability is extremely

valuable in examples such as those depicted in Figures 6 and 8. Lack of or excessive peaks and shoulders were obtained, and what might have been considered poor data was utilized by the man-machine interaction and provided a useful output.

Deconvolution. The optimization algorithm requires an input indicating the nature of the wave shape to be deconvoluted. For the data in Figure 2, the input function is Gaussian, equation (15).

$$Y = \sum_{I=1}^{\text{Num}} XX(I) \exp - \left\{ \text{BETA} [(X - XX(I+1))/XX(I+1)]^{-2} \right\} \quad (15)$$

where X and Y represent smoothed data vectors; XX(I) and XX(I+1) represent storage vectors for spectral peaks, shoulders [XX(I)] and spectral locations [XX(I+1)]; beta is proportional to resolution; and Num is the number of peaks and shoulders to be considered. Comparison of peak No. 4 between Figures 2 and 3, and indeed all the neighboring peaks, shows the improvement resulting from the deconvolution.

The optimization routines can optimize 12 to 20 parameters, depending upon the roundoff error and word length in the computer. On an EMR 6050 computer none of these cases indicated error because of an excessive number of parameters in the algorithm.

The ability to adjust position, intensity, and resolution allows the wave shape to comfortably adjust itself in 3 degrees of freedom to fit the smoothed data vectors. This is indicated in Figures 7 and 8, where the wave shape is expressed by equation (16),

$$Y = Y \max 2^{-\left(\frac{X - X \text{ BAR}}{\text{BETA}}\right)}, \quad (16)$$

and Y max, X BAR, and BETA were optimized. There is good agreement between these results and those of Schwartz [7].

In Figures 12 and 13, two theories were considered, one with all Gaussian wave shapes and another with two Gaussian and one Poisson. For those cases where three peaks were present, both theories were exercised and the criterion function adjusted to fit a Poisson function

for the third peak, equation (17).

$$Y = \sqrt{a} \cdot b \cdot c \exp (-a) \quad (17)$$

where

$$a = (X - X \text{ BAR} + \text{BETA}) / (a_n \cdot \text{BETA})$$

$$b = 1.0/a_n$$

$$c = Y \text{ max} / \sqrt{b} \exp (-b) \quad .$$

The figures represent the deconvolution of three Gaussian or two Gaussian and one Poisson curve. Note the improved fit indicated in the figures and by the final root-mean-square values with the all-Gaussian theory.

The polarimeter data, which required double convolution noise filtering, was curve fit to equation (18),

$$Y = a + b \cos^2 (wt - \phi) \quad . \quad (18)$$

Two cases were considered, one where  $a$ ,  $b$ ,  $w$ ,  $\phi$ , were optimized and a second where  $w$  was predetermined. The resulting polarization compared very favorably with Fourier and synchronous detection methods [9].

## CONCLUSIONS

The application of convolute integers with the multiparameter pattern search lends itself to solving a wide variety of curve-fitting problems. Displaying the output on a graphics terminal allows all the parameters of interest to be considered for a man-machine interaction as the calculations proceed.

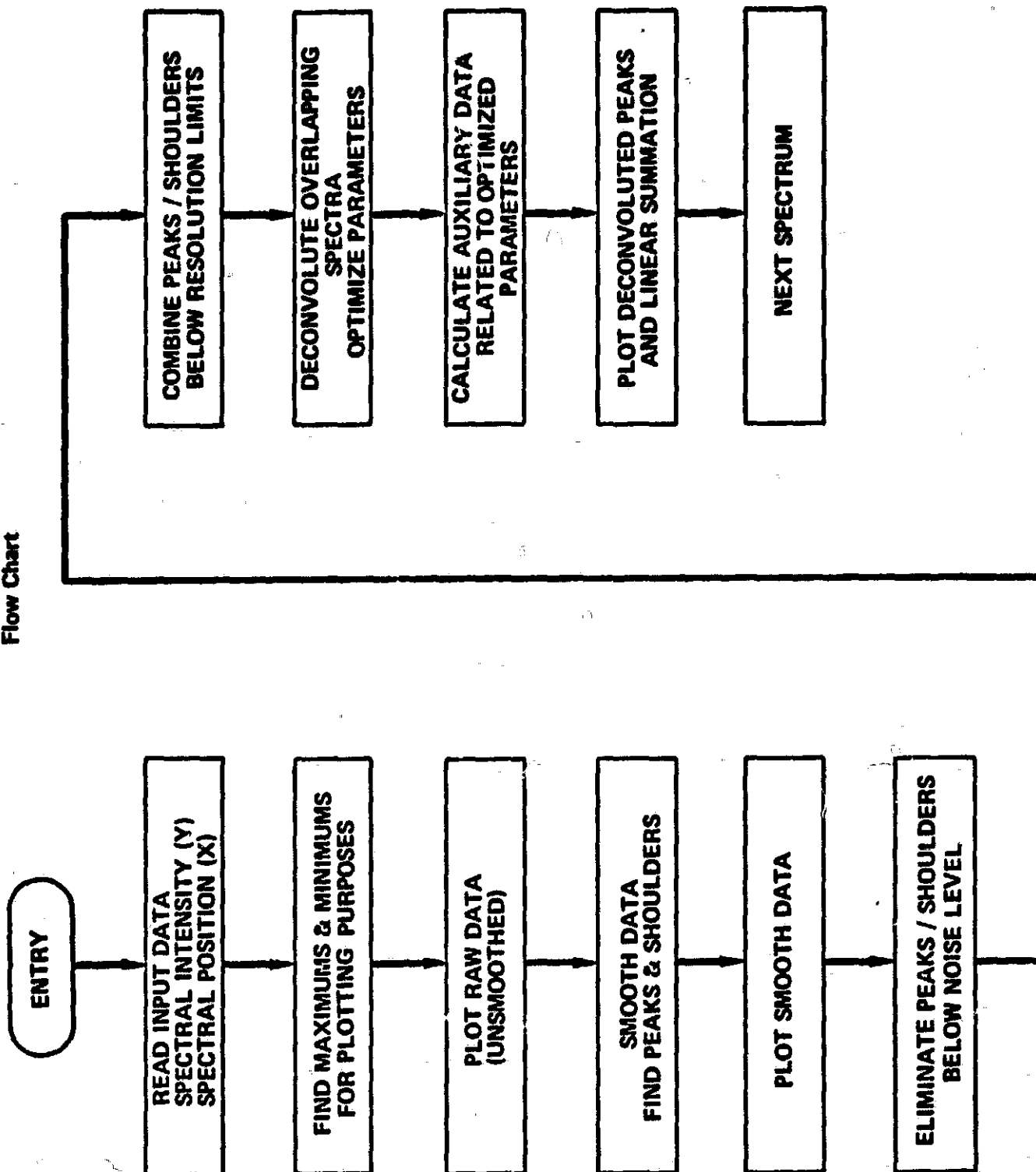
The versatility of the pattern search allows any analytical parameters of interest to be calculated, while the low-pass, high-pass, band-pass characteristics of the convolute integers not only smooth but assist in obtaining initial values for inflection points.

The size of the software would allow use of an 8K minicomputer (16K with a graphics terminal). Time for a solution in some problems can become considerable if initial parameters are in great error, but use of the convolute integer logic has led to rapid convergence; e.g., 30 sec for Figure 13.

As Figures 1 through 13 indicate, the entire software package has provided satisfactory results in a wide variety of problems.

## APPENDIX

Flow Chart



## REFERENCES

1. Horlick, G.: Anal. Chem. 44, 943, 1972.
2. Morrey, J. R.: Anal. Chem. 40, 905, 1968.
3. Jones, R. N.; Venkataraghuran, R.; and Hopkins, J. W.: Spectrochim. Acta. 23A, 925, 1967.
4. Izatt, J. R.; Saki, H.; and Benidict, W. S.: J. Opt. Soc. Am. 59, 19, 1969.
5. Savitzky, A., and Golay, M. J. E.: Anal. Chem. 36, 1627, 1964.
6. Steinier, J., et al.: Anal. Chem. 44, No. 11, 1972.
7. Schwartz, L. M.: Anal. Chem. 43, 1336, 1971.
8. Hooke, R., and Jeeves, T. A.: J. Assoc. Comp. Mach. 8, 212-229, 1961.
9. Gary, G. A.; Craven, P. D.; and Edwards, T. R.: A Comparison of Three Techniques for Reducing Polarimeter Data. IN-ES14-74-3, July 1974 (available from authors).